

## On the Formation of Antarctic Intermediate and Bottom Water in Ocean General Circulation Models

MATTHEW H. ENGLAND\*

*Department of Geology and Geophysics, The University of Sydney, Sydney, Australia*

25 July 1991 and 2 October 1991

### ABSTRACT

A series of coarse-resolution models were integrated with a view to determining the most appropriate representation of the largest-scale water masses formed in the Southern Ocean. In particular, it was hoped that the models could realistically simulate Antarctic Bottom and Intermediate Water. The ocean model employed has a global domain with a realistic approximation of the continental outlines and bottom bathymetry. The subgrid-scale variation of bottom bathymetry is removed by spatial averaging over each grid box. The annual mean forcing at the sea surface is derived from climatological fields of temperature, salinity, and wind stress. It is found that the salinity of shelf water in the Weddell and Ross seas is critical if the model is to appropriately simulate the world's intermediate and bottom water masses. If the surface layer is too fresh in the Weddell and Ross seas, any bottom water formed adjacent to Antarctica is significantly less dense than in the real ocean. Furthermore, surface water at about 60°S (normally the region of intermediate water formation) strongly contributes to the model ocean's bottom water. This leaves the simulated bottom water too fresh and warm. On the other hand, with sufficiently salty bottom-water formed in the extreme Southern Ocean, a low-salinity tongue of intermediate water develops at 60°S. It is suggested that the sea-ice component of climate models is critical if the simulation is to capture the high-salinity shelf water and bottom-water formation adjacent to Antarctica and, in turn, allow for a realistic tongue of low-salinity Antarctic Intermediate Water (AAIW). The bathymetry of the Drake Passage is shown to determine the shape and strength of an intense meridional overturning cell in the Southern Ocean. By properly representing the northward extent of the Drake Passage, the formation and equatorward spreading of AAIW is simulated realistically. The scheme of AAIW formation obtained is quite different from the classical notion of circumpolar subduction of surface water at the polar front.

### 1. Introduction

This note describes a series of coarse-resolution World Ocean models that were integrated with a view to determining the most appropriate representation of the global-scale water masses formed in the Southern Ocean. Because the global balance of heat and fresh-water is closely related to the formation of the world's water masses, this study has particular relevance to numerical investigations of global climate. For this reason, the ocean model employed was chosen to be one that has often been coupled to numerical models of the atmosphere in order to study global climate (e.g., Stouffer et al. 1989; Manabe et al. 1991). The ocean model is a version of the multilevel numerical model described by Bryan (1969) and adapted to modern vectorizing computers by Cox (1984) and Pacanowski et al. (1991) at the Geophysical Fluid Dynamics Laboratory (GFDL). A similar investigation was reported by Cox (1989) with an idealized geometry and surface

boundary conditions. In the present study, we use realistic geometry and extend the analysis to include the role of salinity forcing off Antarctica and the importance of the bathymetry of the Drake Passage. In more recent experiments, we investigate the sensitivity of the model to variations in the rate of geopotential mixing of tracers, as well as quantify the role of the Indonesian throughflow on the simulated circulation and check the ability of the model to represent more than one source of deep water (England 1992).

Hydrographic observations of temperature and salinity in the Southern Ocean indicate that the region is characterized by the formation of two global-scale water masses: one so dense that it sinks to the bottom of the World Ocean, the other only dense enough to sink to intermediate depths (for example, see Levitus 1982). The denser water mass, known as Antarctic Bottom Water (AABW), is formed in the extreme Southern Ocean during austral winter when the ocean releases heat into the atmosphere and when sea-ice formation rejects salt into the water column. Both these effects leave the seawater extremely dense, for it is both colder and saltier than usual. AABW is characterized by a temperature-salinity signature of roughly 0°C and 34.70 psu (Carmack 1986). The other major Southern Ocean water mass is known as Antarctic Intermediate

\* Current affiliation: UMR 39, CNES/ARAS, Toulouse, France.

Corresponding author address: Dr. Matthew H. England, Department of Geology and Geophysics, The University of Sydney, Sydney, Australia.



Water (AAIW) and it also tends to be formed during the Southern Hemisphere winter (Deacon 1937). It is characterized by a relatively low-salinity tongue (about 34.4 psu) that sinks at about 60°S and spreads equatorward at about 1000-m depth (see Fig. 2a). It was first suggested (e.g., Sverdrup et al. 1942, p. 619) that AAIW formation occurs circumpolarly by cross-polar-frontal mixing of low salinity Antarctic surface water and sub-Antarctic surface water.

Unfortunately, many climate models have failed to accurately represent the water-mass structure in the Southern Hemisphere (e.g., Manabe and Stouffer 1988; Washington and Meehl 1989; Mikolajewicz and Maier-Reimer 1990; Manabe et al. 1991). Furthermore, a deep meridional overturning cell under the polar westerlies is a feature common to the simulated circulation in some of these models. This cell suggests intense diapycnal advection through the region normally characterized by equatorward spreading of AAIW. It has been suggested that the cell is an artifact of the geopotential mixing of tracers employed by coarse-resolution models (McDougall and England 1992). To strengthen the debate, this deep ventilating cell is important in slowing down the simulated climate response to a gradual increase in atmospheric CO<sub>2</sub> (e.g., Stouffer et al. 1989; Manabe et al. 1991). One of the central goals of this study is to determine whether a purely prognostic version of the GFDL Ocean General Circulation Model (OGCM) can properly represent water-mass formation in the Southern Hemisphere with only coarse horizontal and vertical resolution.

One notable study that successfully captures the water-mass structure of the World Ocean is the simulation conducted by Bryan and Lewis (1979). Although not mentioned explicitly in their report, they capture AAIW by enhancing the salinity in the immediate vicinity of the Antarctic continent. Interestingly, their Southern Ocean meridional overturning cell reveals an equatorward mass transport at about 1000-m depth (see their Fig. 10a), corresponding to where the simulated AAIW resides. In this sense, their midlatitude salinity structure is a good tracer of the modeled ocean circulation. In the present study, we capture AAIW formation without producing a corresponding equatorward flow in the zonally integrated mass transport.

The OGCMs that have been most successful at capturing the large-scale water-mass distribution in the Southern Ocean (e.g., Semtner and Chervin 1988; Saunders and Thompson 1992) have tended to be "semidiagnostic" (or "robust diagnostic"), in that some of the interior model grid points have their temperatures and salinities restored toward observed values. In such models, the intermediate and deep water masses need not be formed at the surface by convective overturning; they can originate unrealistically from those interior grid points being relaxed to observations. Toggweiler et al. (1989) found that a purely prognostic version of the GFDL OGCM produced a deep ocean

circulation superior to a semidiagnostic realization because the weak interior restoring terms tend to suppress convection and other vertical motions. In modeling global climate, it is important to represent realistically the ventilation processes in the World Ocean. This study employs a purely prognostic OGCM to model the major water masses of the World Ocean, in that only the surface thermohaline field is relaxed to climatological conditions.

## 2. The World Ocean experiments

The ocean model employed in this study is the Pacanowski et al. (1991) version of the GFDL OGCM. The model has a global coverage of the ocean, with a realistic approximation of bottom bathymetry and continental boundaries. The grid spacing is chosen to be 4.5° latitude by 3.75° longitude with 12 vertical levels, matching the resolution used in the standard GFDL climate model. Because of the coarse horizontal and vertical resolution, the effects of mesoscale eddies are only taken into account implicitly by approximate closure schemes. The mixing of tracers takes place in Cartesian coordinates at a rate that is depth dependent (similar to Bryan and Lewis 1979). In more recent experiments, we employ a weak background Cartesian mixing (for numerical stability), and incorporate an isopycnal mixing scheme (Redi 1982; Cox 1987) that more realistically represents the tendency for heat and salt to be mixed on surfaces of constant density. The ocean is forced at the sea surface by climatological boundary conditions of temperature, salinity, and wind stress. While the effects of seasonal variations in the freshwater balance are artificially represented in the extreme Southern Ocean in some of the experiments, the model is generally forced by the observed annual mean conditions reported by Levitus (1982) and Hellerman and Rosenstein (1983). In future experiments, we plan to incorporate seasonal variations in the observed fluxes of heat, freshwater, and momentum into the model.

Figure 1 shows a chronology of the numerical experiments studied thus far, as well as an indication of other integrations presently being investigated. The steady states denoted in the figure correspond to a model ocean with negligible long-term drift in the temperature, salinity, and circulation fields. Only experiments I and II are spun up from an initially isothermal ocean at rest with uniform salinity. The other cases follow on from steady or quasi-steady states obtained in previous experiments. When there is a change in topography from one case to the next (e.g., from experiment IIIa to IIIb), the temperature and salinity fields are held constant while the velocity field adjusts to the new continental boundaries. After this initial adjustment process, the integration proceeds as usual.

Although some fascinating results appear in the cases with only a thermohaline component in the circulation



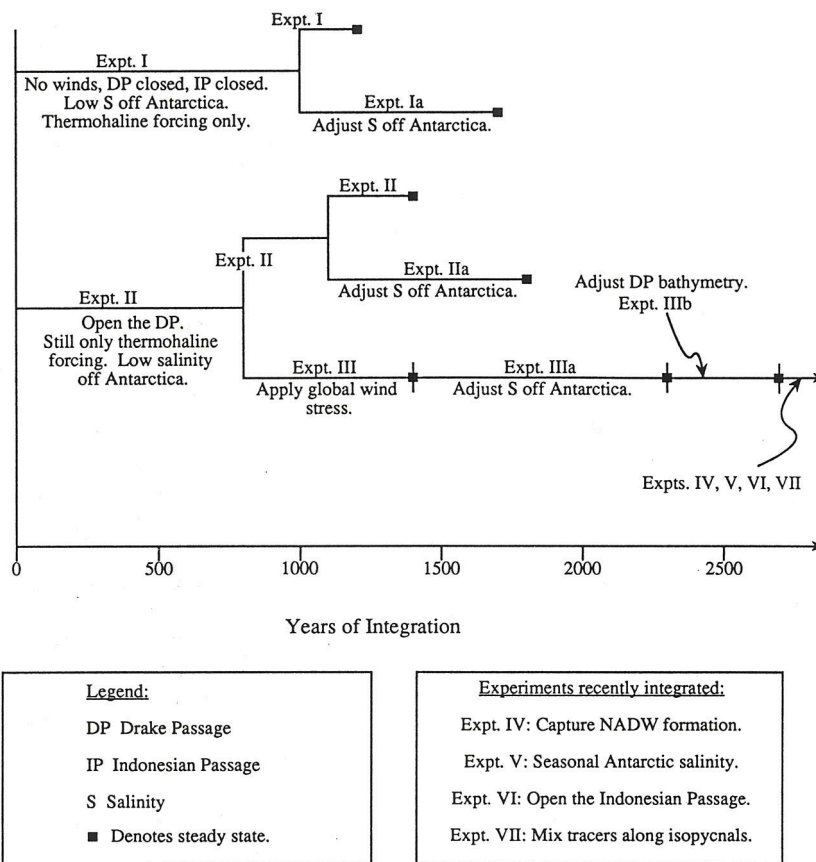


FIG. 1. Time series of the World Ocean experiments. The integration time corresponds with the number of years of effective surface integration. The bottom layers of the model are effectively integrated for much longer times through the vertical acceleration technique of Bryan (1984).

(i.e., with no surface wind stress), this note will concentrate on the results obtained in experiments III, IIIa, and IIIb. These experiments are all forced by surface boundary conditions that vary only with latitude, corresponding simply to the zonal average of observed temperature, salinity, and wind stress. For this reason, surface salinities in the North Atlantic and North Pacific are roughly the same (less than 34.0 psu) and too fresh for any deep-water formation. The simulation of North Atlantic Deep Water formation will come in experiment IV, when a distinction is made between the relative saltiness of the North Atlantic and the freshness of the North Pacific. For now, experiments III, IIIa, and IIIb are useful for evaluating the representation of water-mass formation in the Southern Hemisphere, where properties at the surface are predominantly zonal.

The surface heat and freshwater fluxes forcing experiment III are implied by restoring the surface temperature and salinity to a zonal average of Levitus' (1982) annual mean climatology. In the extreme Southern Ocean, the annual mean salinity reported by Levitus (1982) is based on few measurements and is biased toward summertime observations, when sea-ice

melt leaves the region relatively fresh. In fact, when sea ice is formed during winter there is no chance of ships measuring the high-salinity shelf water in the Ross and Weddell seas with conventional hydrographic instruments. So, it turns out that experiment III is too fresh in the extreme Southern Ocean to form realistically saline deep water. This has been a problem with other ocean general circulation models forced at the sea surface by annual mean Levitus (1982) climatology (e.g., Toggweiler et al. 1989). It is also a problem with coupled ocean-atmosphere models with annual mean insolation of the earth's fluid envelope (England et al. 1992). For example, Fig. 2 compares observed salinity in the Pacific Ocean with that simulated in the annually insulated climate model of Manabe and Stouffer (1988). The simulated salinity structure is quite different from the observed field, particularly in the Southern Ocean. In spite of a surface freshwater flux correction term, the near-surface water adjacent to Antarctica is unrealistically fresh (less than 33.5 psu), with an intense halocline prohibiting any bottom-water formation in the region. Instead, water at about 60°S (normally the latitude of intermediate water formation) sinks and forms the model ocean's bottom water

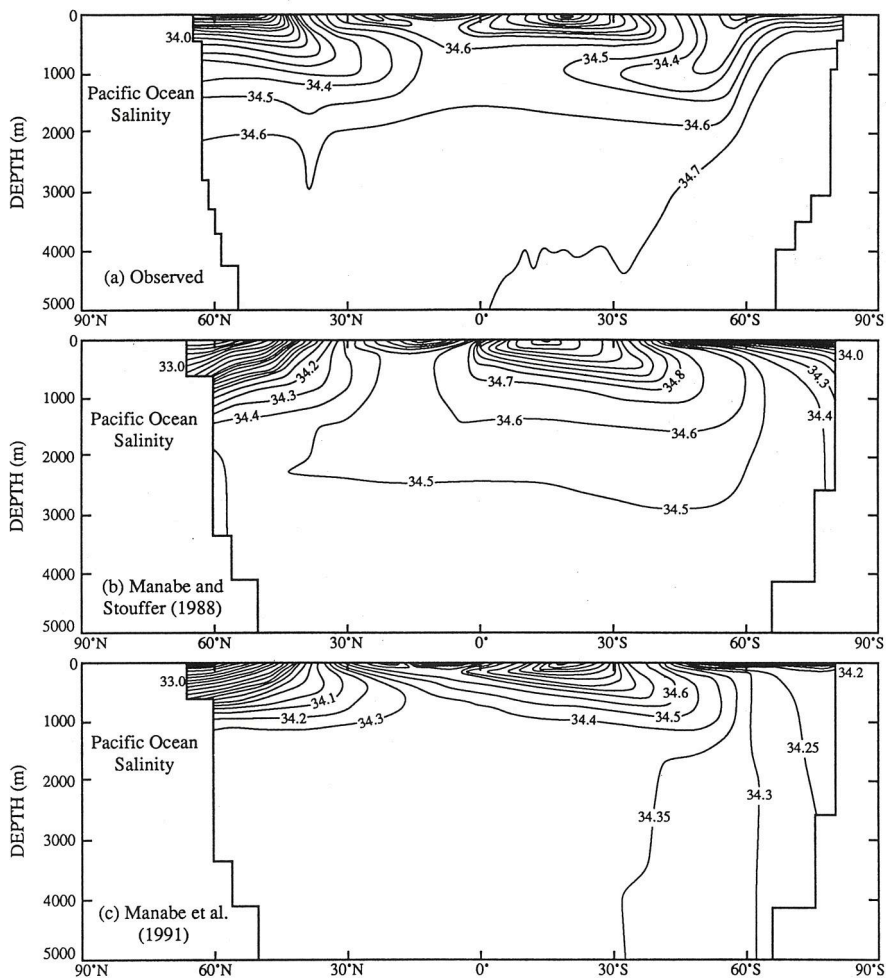


FIG. 2. Zonally averaged and annually averaged latitude–depth sections of salinity in the Pacific Ocean. (a) Observed (redrafted from Levitus 1982), (b) in the Manabe and Stouffer (1988) climate model (their experiment I), and (c) in the Manabe et al. (1991) seasonally insulated climate model.

(England et al. 1992). This leaves the simulated deep ocean too fresh and warm. Because the model has no seasonal insolation, the wintertime water-mass formation processes are not represented, and the resulting salinity structure is very unrealistic. Manabe et al. (1991) improve the representation of deep and intermediate salinity by imposing the seasonally varying insolation at the top of their model atmosphere. However, their bottom water is still too fresh (less than 34.5 psu), and their AAIW has an unrealistic structure (see their Fig. 7), particularly in the Pacific Ocean (Fig. 2c).

In order to evaluate the role of wintertime AABW formation in determining the world's water-mass distribution, experiment IIIa was integrated with an imposed high surface salinity adjacent to Antarctica (south of 65°S). The southernmost row of ocean grid points is restored toward a maximum value of 35.0 psu, with a smooth interpolation defining the enhanced

forcing at the remaining latitudes up to 65°S. The maximum surface salinity chosen matches estimates of the wintertime salinity of shelf water in the Ross and Weddell seas (Foster and Carmack 1976) when sea-ice formation rejects salt into the water column, leaving the seawater quite saline (up to 35.0 psu). This process tends to be confined to localized regions off Antarctica (Grumbine 1991), making convection the important process forming AABW. Here we approximate this subgrid-scale process by restoring surface salinities toward typical wintertime values, as if sea ice were present. So, although the experiment is run with time-invariant annual mean boundary conditions, there is a perpetual winter surface salinity imposed in the extreme Southern Ocean. This contrasts with experiment III, where there is an effective surface forcing toward fresh *summertime* conditions due to the relaxation toward Levitus (1982) climatology. In more recent experiments the salinity forcing in the Southern



Ocean has a time dependence, with fresh surface conditions for most of the year and only a 3-month wintertime salinity enhancement (England 1992). This further improves the representation of Southern Hemisphere water masses reported here.

Finally, the role of the Drake Passage bathymetry is studied in experiment IIIb by adjusting the model's continental boundaries so that the ocean's "barrier-free zone" is more realistically poleward of the maximum westerly wind belt. The conventional GFDL climate model has an artificially wide Drake Passage that infringes on the latitudes of strong westerly wind stress, forcing deep meridional overturning to compensate near-surface Ekman transport (e.g., Toggweiler et al. 1989; Stouffer et al. 1989; Manabe et al. 1991). The resulting ventilation of the deep ocean in this region significantly moderates the simulated climate response to a gradual increase in atmospheric  $\text{CO}_2$  (e.g., Stouffer et al. 1989). By better representing the Drake Passage bathymetry (in particular, by shifting the gap poleward), we extend the region where a significant zonal

pressure gradient can exist. In this case, more of the near-surface Ekman transport can be balanced by geostrophic return flow in the upper ocean, and the deep ventilation will weaken.

### 3. World Ocean model results

Figures 3 and 4 show the zonally averaged salinity and meridional overturning in experiments III, IIIa, and IIIb. In experiment III, all of the World Ocean deep water is formed in the Southern Ocean (remembering the unrealistic freshness of the North Atlantic at this stage in the experiments). The formation of the deep water occurs at two distinct latitude bands; one adjacent to Antarctica, the other associated with the deep overturning cell driven by the circumpolar westerlies (recently termed the "Deacon cell"). Furthermore, the water adjacent to Antarctica is dense, primarily through its temperature, so that the marginally saltier surface water at  $60^\circ\text{S}$  can also be transported deep into the ocean. Normally the water at  $60^\circ\text{S}$  would

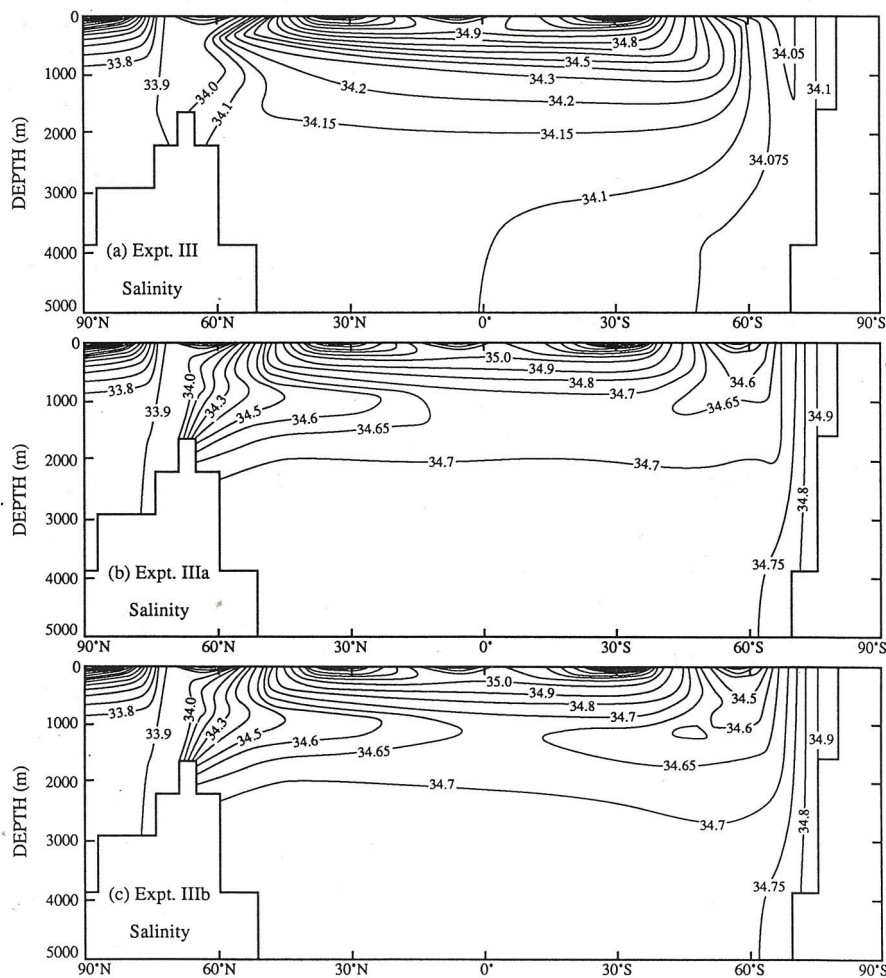


FIG. 3. Globally averaged latitude-depth sections of salinity in experiments III, IIIa, and IIIb.

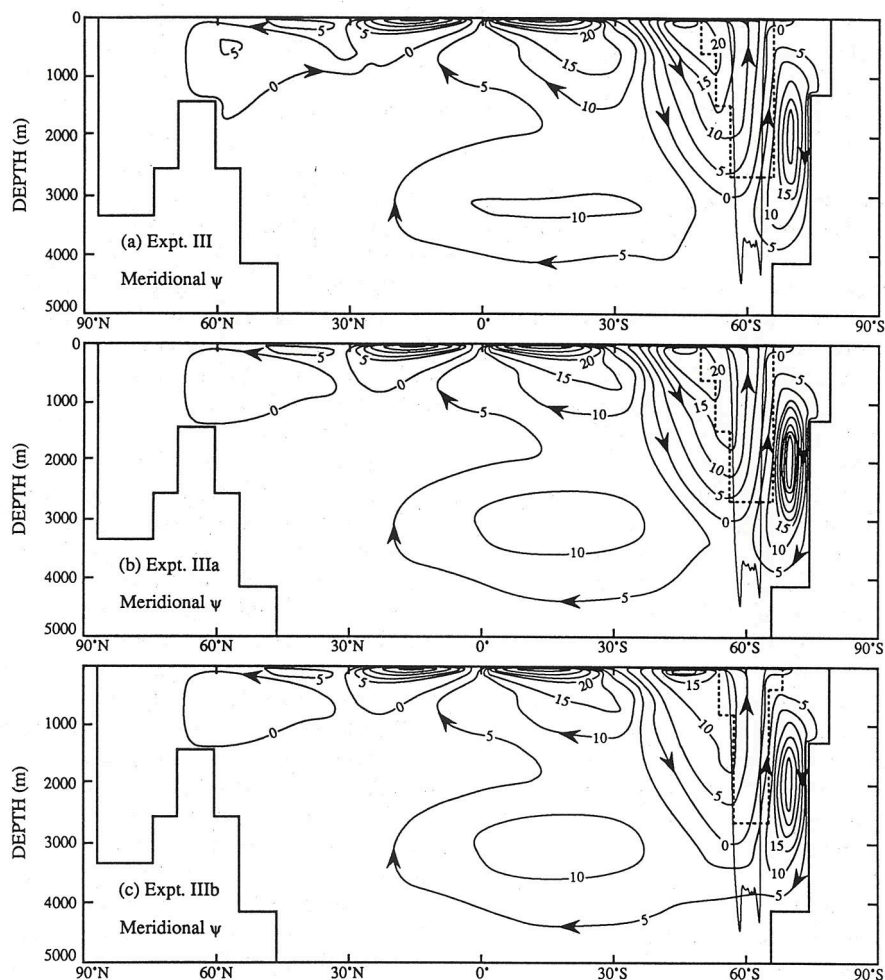


FIG. 4. Globally averaged mass transport in the meridional plane in experiments III, IIIa, and IIIb. The dashed contour near 60°S denotes the model's representation of the Drake Passage in each experiment, whereas the fine contour shows the actual Drake Passage bathymetry.

form a low-salinity tongue of intermediate water (Fig. 2a). The problem with experiment III in terms of the lack of AAIW formation appears to be twofold. One factor is that the bottom water formed adjacent to Antarctica is not dense enough (through its relative freshness) to provide a limit to the intermediate water sinking. Instead, the "would-be" intermediate water sinks to great depths, for it never encounters a dense enough water mass to keep it buoyant. The second factor is the presence of the deep wind-driven Deacon cell, which transports intermediate water to great depths. The shape of the Deacon cell turns out to be strongly determined by the bathymetry of the Drake Passage gap (Fig. 4), so it could be that the unrealistic shape of the Drake Passage is inhibiting AAIW formation. Notice also the very *weak* intermediate water formation in the Northern Hemisphere in experiment III (Fig. 3a). Given that both Northern Hemisphere basins are forced by relatively fresh surface salinities, we hope to

simulate North Pacific Intermediate Water (NPIW) accurately. However, it turns out that the Northern Hemisphere intermediate water is only marginally more buoyant than the modeled bottom water in experiment III.

By imposing winter salinity conditions in the extreme Southern Ocean, the salinity structure in experiment IIIa becomes dramatically different, even though the meridional overturning in the model is essentially unchanged from experiment III. With high salinity shelf water formed in the Ross and Weddell seas, the model's bottom water is now formed *exclusively* adjacent to Antarctica. Furthermore, there is intermediate water formation in both hemispheres, particularly in the Northern Hemisphere. With sufficiently dense bottom water in the model ocean, the low-salinity tongues of AAIW and NPIW only sink to intermediate levels, then spread equatorward. However, it does seem that the AAIW is still somewhat hindered by the strong Deacon



cell (something its Northern Hemisphere counterpart does not have to deal with), which would tend to erode the equatorward propagating tongue of low salinity.

The figures showing meridional overturning include a contour representing the real and modeled Drake Passage bathymetry. In order to resolve the Antarctic Circumpolar Current in the model, the Drake Passage needs to be artificially wide (at least two velocity grid points are needed to produce a realistic throughflow). However, by making it wide and, in particular, by extending the gap into the latitudes of strong westerly winds, the model tends to exaggerate the presence of the Deacon cell. In experiment IIIb, with only a moderate change in the Drake Passage bathymetry, the Deacon cell becomes significantly weaker at intermediate levels. This is because there is now a more realistic meridional barrier to allow shallow return flow under the surface Ekman currents. The effect this change in the Deacon cell has on the salinity structure is quite dramatic. There is now realistic equatorward spreading of the low-salinity tongue of AAIW. If the model resolution was adequate to properly resolve the Drake Passage throughflow without artificially widening the gap, the representation of AAIW may improve further. It turns out that the simulation of AAIW is even more realistic when the mixing of heat and salt takes place on isopycnal surfaces (thereby allowing a decrease in the rate of horizontal diffusion) and when the surface boundary conditions have their observed zonal variability (England 1992).

One consequence of enhancing the salinity adjacent to Antarctica is that the rate of formation of AABW increases dramatically (Fig. 4). Bryan and Lewis (1979) find that their model ocean bottom water is too cold by 1°–2°C, owing to the strength of AABW formation driven by the increased Antarctic salinities. Table 1 presents the globally averaged temperature–salinity profile simulated in experiment IIIb, as well as

the corresponding profile interpolated from the annually and globally averaged Levitus (1982) climatology. The correspondence between observed and simulated mean profiles is quite good on the whole. As in other coarse-resolution ocean GCMs, the permanent subtropical thermocline is too thick. The simulated bottom water is only marginally too cold, which is probably linked to the absence of any warm NADW in experiment IIIb. The intermediate salinity minimum is well represented in the globally averaged profile, even though there is no equivalent of salty NADW in experiment IIIb. This indicates that our intermediate water is a little too saline, for the introduction of NADW will enhance the intermediate and deep salinity field.

As a final point to this note, it is interesting to trace the renewal processes of AAIW in the model. Figure 5a shows the salinity at 755-m depth (level 6 of the ocean model) in experiment IIIb. From this figure and a preliminary analysis of the salt budget in experiment IIIb, it seems as though the AAIW is renewed in two principal locations, even though the low-salinity tongue is a feature of each ocean basin. The major source appears to be in the far southwest Atlantic just north of the Drake Passage throughflow, where strong downwelling transports 34.4 psu water into the ocean interior (Fig. 5b). From there, the low-salinity tongue is transported zonally into the Indian Ocean. The other principal source is in the southeast Pacific Ocean off the coast of southern Chile, from where northward advection transports the intermediate water equatorward. This picture of AAIW formation is quite different from the traditional notion of circumpolar cross-frontal mixing and consequent subduction of Antarctic and sub-Antarctic surface water, though it coincides with the renewal process proposed by McCartney (1977).

#### 4. Conclusions

It has been shown that the salinity of shelf water in the extreme Southern Ocean is critical if ocean models are to appropriately simulate the world's intermediate and bottom water masses. If the surface layer is too fresh in the Weddell and Ross seas, any bottom water formed adjacent to Antarctica is significantly less dense than in the real ocean. Furthermore, surface water at about 60°S (normally the region of intermediate water formation) strongly contributes to the model ocean's bottom water. This leaves the simulated bottom water too fresh and warm.

With an increased surface salinity in the Ross and Weddell seas, however, the model's bottom water becomes realistically saline and dense. Furthermore, low-salinity tongues of intermediate water are formed in each hemisphere because the now dense deep layers of the ocean provide a limit to their sinking. This suggests that the reason many climate models fail to capture intermediate water formation, in spite of having sea-

TABLE 1. Globally averaged temperature–salinity profile simulated in experiment IIIb, as well as the corresponding profile interpolated from the annually and globally averaged Levitus (1982) climatology. Temperature ( $T$ ) values are given in degrees Celsius, and salinity ( $S$ ) in practical salinity units (psu).

Depth (m)	$T$ (obs)	$T$ (IIIb)	$S$ (obs)	$S$ (IIIb)
1 25.45	17.78	17.81	34.77	34.84
2 85.10	15.59	15.73	34.99	34.92
3 169.50	12.68	13.83	35.01	34.88
4 295.25	9.93	11.58	34.87	34.78
5 482.80	7.54	9.24	34.69	34.68
6 754.60	5.35	6.81	34.60	34.60
7 1130.65	3.69	4.75	34.63	34.61
8 1622.40	2.67	2.89	34.70	34.65
9 2228.35	1.97	1.46	34.74	34.69
10 2934.75	1.51	0.89	34.74	34.72
11 3720.90	1.16	0.65	34.73	34.73
12 4565.55	0.91	0.60	34.73	34.74



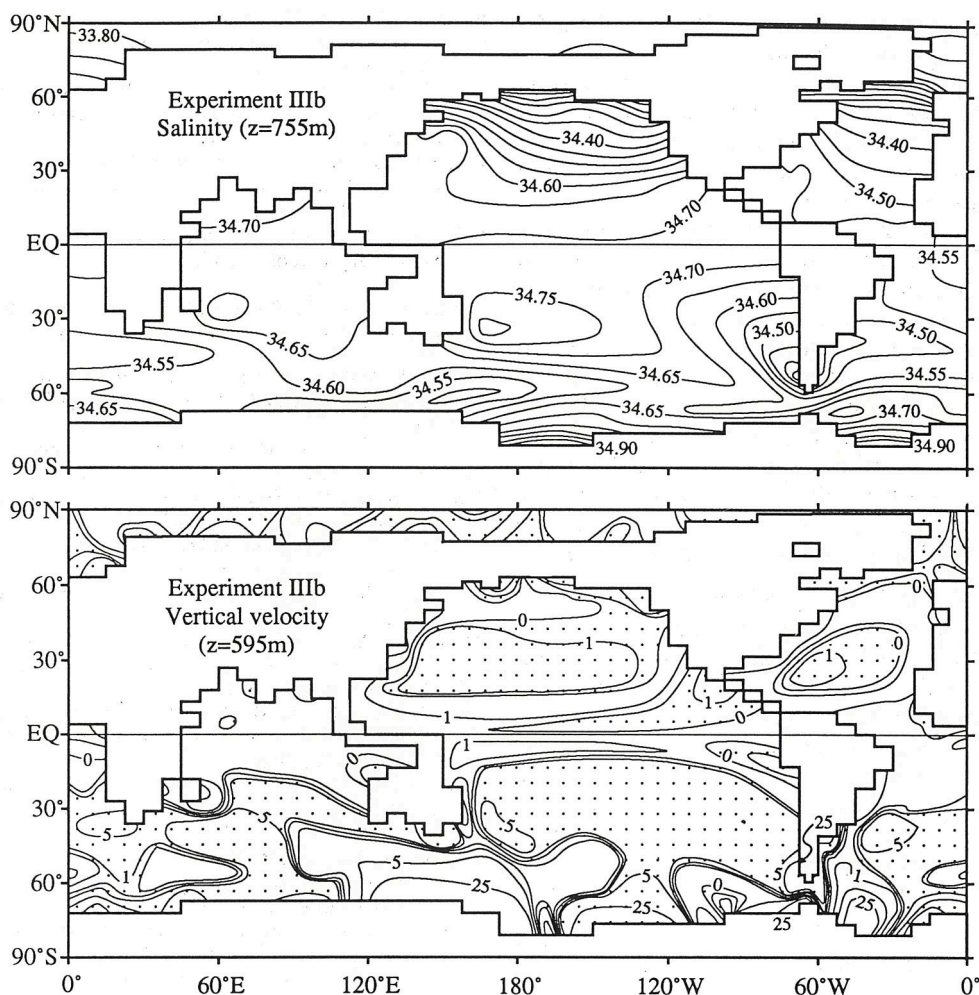


FIG. 5. (a) Salinity at 755-m depth (level 6 of the ocean model) in experiment IIIb. (b) Vertical velocity distribution ( $\text{cm day}^{-1}$ ) at 595-m depth in experiment IIIb. In the stippled areas, vertical motions are downward. Contours are drawn at 0, 1, 5, and  $25 \text{ cm day}^{-1}$ .

sonal insolation at the top of the model atmosphere (e.g., Manabe et al. 1991), lies in the unrealistically consistent freshness of surface water in the extreme Southern Ocean. This could have to do with the sea-ice component in these models, for the rejection of salt into the water column as sea ice forms is the principal process to increase surface salinities in the extreme Southern Ocean. However, it may be due entirely to the freshwater flux adjustment term, for this is derived in part from the seasonal salinity data of Levitus (1986), which is too fresh at the high latitudes of the Southern Hemisphere during winter. So, even though the surface salinity is enhanced as sea ice forms in the model, the change in salinity may be compensated entirely by the freshwater flux adjustment toward climatological conditions.

The bathymetry of the Drake Passage was shown to determine the shape and strength of an intense merid-

ional overturning cell in the Southern Ocean. By properly representing the northward extent of the Drake Passage, the formation and equatorward spreading of AAIW is simulated realistically. Surprisingly, this means that on a *zonal average* at least, the low-salinity tongue of AAIW and the ventilating Deacon cell coexist. Figure 5b shows a map of the vertical velocity between levels 5 and 6 (i.e., at 595-m depth) in experiment IIIb. This map reveals the distribution of downward advection associated with the overturning cell shown in Fig. 4c. In particular, the downward component of the Deacon cell corresponds with the broad region of downwelling found at virtually all longitudes between 30° and 50°S. Notably strong downwelling is apparent on either side of the southern tip of South America, corresponding to the salinity minima shown in Fig. 5a. From a comparison of Figs. 5a and 5b, it seems as though the Deacon cell advects



downward through the tongue of AAIW in each ocean basin. However, a salt-budget analysis reveals that it is primarily horizontal diffusion that erodes the AAIW. This result is confirmed in a recent integration with decreased horizontal diffusion coefficients (England 1992) in which the AAIW tongue freshens by several tenths of a part per thousand.

As a positive result for those who believe that the Deacon cell is a realistic aspect of the circulation in the Southern Ocean, this study shows how the low-salinity tongue of AAIW does not necessarily define the zonally averaged particle motion in the Southern Ocean. On the other hand, this study also shows that a less intense ventilation of the deep ocean under the polar westerlies allows a more realistic equatorward spreading of the low salinity water mass. Further modeling and analysis is being directed at an understanding of the physical processes forming and maintaining AAIW in such a coarse-resolution prognostic OGCM.

**Acknowledgments.** The World Ocean models were run on the CSIRO Y-MP Cray with the financial support of a CSIRO INRE Postgraduate Project Award. The author is indebted to Kirk Bryan for accommodating an invaluable visit to the GFDL during September 1990 and to Keith Dixon for providing a copy of the GFDL Modular Ocean Model. Matthias Tomczak suggested the salinity adjustment off Antarctica and gave a helpful review of the original manuscript. Ron Stouffer kindly provided data from the Manabe and Stouffer (1988) and Manabe et al. (1991) climate models.

#### REFERENCES

- Bryan, K., 1969: A numerical method for the study of the circulation of the World Ocean. *J. Comput. Phys.*, **3**, 347–376.
- , 1984: Accelerating the convergence to equilibrium of ocean-climate models. *J. Phys. Oceanogr.*, **14**, 666–673.
- , and L. J. Lewis, 1979: A water mass model of the World Ocean. *J. Geophys. Res.*, **85**(C5), 2503–2517.
- Carmack, E. C., 1986: Circulation and mixing in ice covered waters. *The Geophysics of Sea Ice*, N. Untersteiner, Ed., Plenum, 641–712.
- Cox, M. D., 1984: A primitive equation, three-dimensional model of the ocean. GFDL Ocean Group Tech. Rep. No. 1, 143 pp.
- , 1987: Isopycnal diffusion in a z-coordinate ocean model. *Ocean Modelling*, **74**, 1–5.
- , 1989: An idealized model of the World Ocean. Part I: The global scale water masses. *J. Phys. Oceanogr.*, **19**, 1730–1752.
- Deacon, G. E. R., 1937: The hydrology of the Southern Ocean. *Discovery Reports*, Cambridge University Press, **15**, 1–124.
- England, M. H., 1992: On the formation of the global-scale water masses in ocean general circulation models. *J. Phys. Oceanogr.*, **22**, submitted.
- , M. Tomczak, and J. S. Godfrey, 1992: Water-mass formation and Sverdrup dynamics; a comparison between climatology and a coupled ocean-atmosphere model. *J. Mar. Systems*, **3**, in press.
- Foster, T. D., and E. C. Carmack, 1976: Frontal zone mixing and Antarctic bottom water formation in the southern Weddell Sea. *Deep-Sea Res.*, **23**, 301–317.
- Grumbine, R. W., 1991: A model of the formation of High Salinity Shelf Water on polar continental shelves. *J. Geophys. Res.*, **96**, 22 049–22 062.
- Hellerman, S., and M. Rosenstein, 1983: Normal monthly wind stress over the World Ocean with error estimates. *J. Phys. Oceanogr.*, **13**, 1093–1104.
- Levitus, S., 1982: *Climatological Atlas of the World Ocean*. NOAA Prof. Paper 13, U.S. Dept. of Commerce, Washington, DC, 173 pp.
- , 1986: Annual cycle of salinity and salt storage in the World Ocean. *J. Phys. Oceanogr.*, **16**, 322–343.
- Manabe, S., and R. J. Stouffer, 1988: Two stable equilibria of a coupled ocean-atmosphere model. *J. Climate*, **1**, 841–866.
- , M. J. Spelman, and K. Bryan, 1991: Transient responses of a coupled ocean-atmosphere model to gradual changes of atmospheric CO<sub>2</sub>. Part I: Annual mean response. *J. Climate*, **4**, 785–818.
- McCartney, M. S., 1977: Subantarctic Mode Water. Contribution to *George Deacon: 20th Anniversary Volume*, M. V. Angel, Ed., Pergamon Press, 103–119.
- McDougall, T. J., and M. H. England, 1992: Horizontal mixing in the Antarctic Circumpolar Current and the Deacon cell. *J. Phys. Oceanogr.*, **22**, submitted.
- Mikolajewicz, U., and E. Maier-Reimer, 1990: Internal secular variability in an ocean general circulation model. *Clim. Dyn.*, **4**, 145–156.
- Pacanowski, R. C., K. W. Dixon, and A. Rosati, 1991: GFDL Modular Ocean Model, Users Guide Version 1.0, GFDL Ocean Group Tech. Rep. No. 2, 46 pp.
- Redi, M. H., 1982: Oceanic isopycnal mixing by coordinate rotation. *J. Phys. Oceanogr.*, **12**, 1154–1158.
- Saunders, P. M., and S. R. Thompson, 1992: Transport, heat and freshwater fluxes within a diagnostic numerical model (FRAM). *J. Phys. Oceanogr.*, **22**, submitted.
- Semtner, A. J., and R. C. Chervin, 1988: A simulation of the global ocean circulation with resolved eddies. *J. Geophys. Res.*, **93**, 15 502–15 522.
- Stouffer, R. J., S. Manabe, and K. Bryan, 1989: Interhemispheric asymmetry in climate response to a gradual increase of atmospheric CO<sub>2</sub>. *Nature*, **342**, 660–662.
- Sverdrup, H. U., M. W. Johnson, and R. H. Fleming, 1942: *The Oceans: Their Physics, Chemistry and General Biology*. Prentice-Hall, 1087 pp.
- Toggweiler, J. R., K. Dixon, and K. Bryan, 1989: Simulations of radiocarbon in a coarse-resolution world ocean model. I: Steady state prebomb distributions. *J. Geophys. Res.*, **94**, 8217–8242.
- Washington, W. M., and G. A. Meehl, 1989: Climate sensitivity due to increased CO<sub>2</sub>: Experiments with a coupled atmosphere and ocean general circulation model. *Clim. Dyn.*, **4**(1), 1–38.